Modeling Negative Temperature Coefficient region in methane oxidation

Pino Sabia [a], Mara de Joannon [a,*], Antonio Picarelli [b], Alfonso Chinnici [a,b], Raffaele Ragucci [a]

[a] Istituto di Ricerche sulla Combustione, C.N.R., Piazzale Tecchio, n°80, 80125 Naples, Italy
[b] Dipartimento di Ingegneria Chimica, Università Federico II, Piazzale Tecchio, n°80, 80125 Naples, Italy

ARTICLE INFO

ABSTRACT

Standard kinetic models are essential tools for predicting and interpreting the evolution of oxidation processes and obtain useful information for designing and dimensioning practical combustion facilities. Quite often a large part of the development work consists in the determination of the most suited chemical kinetics scheme to use in numerical simulations. This step is even more critical in the case of innovative technologies. In fact, in this case, models are required to work in extrapolative conditions, i.e. in range of parameters outside the ones for which they have been optimized. This is the case of prediction methane autoignition at atmospheric pressure, in diluted conditions, corresponding to MILD combustion conditions, where no experimental data are available. The aim of the present work is to compare the efficacies in predicting the existence of Negative Temperature Coefficient (NTC) behavior of ignition time of methane at atmospheric pressure of several kinetic models available in the literature. Such phenomenology is extensively described in the literature for high molecular weight paraffin but few experimental evidences are reported about its occurrence in methane oxidation. Methane autoignition time in dependence of temperature, reaction pathways with rate of production, sensitivity and flow diagram analysis have been exploited in order to highlight the kinetic controlling steps of methane autoignition at different temperature ranges. It has been shown that the prevalence of either the oxidation or the recombination results in a speeding or a slowing down of the reactive process. In this reactive network, a key role is covered by the active oxidation pathway. At the same time, in dependence of working temperature, the branching routes of H_2/O_2 reaction mechanism supply a great part of radicals needed for ignition. Thus, numerical results presented in the paper clearly show that the Negative Temperature Coefficient region in the Arrhenius plot of methane ignition delay marks the shift from one principal reaction route to the others.

© 2011 Elsevier Ltd. All rights reserved.

1. Introduction

Evaluation of reactive processes by means of standard kinetic models is an essential tool for designing practical facilities especially for innovative technologies. In this perspective very often available models are required to work in extrapolative conditions because they have to predict behaviors in range of parameters where sparse or no experimental data are available for the tuning of mechanisms themselves. For instance, this is the case of novel combustion processes, such as MILD [1,2] and oxyfuel [3] combustion. They work in diluted, preheated conditions thus shifting the concentration and temperature ranges of interest outside the boundaries considered in standard applications. The above mentioned lack of experimental data affects the robustness and the reliability of kinetic mechanism to be used in design and dimensioning of practical devices to be operated in these specific conditions. An acceptable evaluation of the effectiveness of kinetic

models in such working conditions can derive from the comparison among results obtained by simulation of specific processes that are particularly sensitive to the prevalence of one or more of the different kinetic pathways involved in hydrocarbon oxidation kinetics. For instance this is the case of fuel auto-ignition which is strongly affected by competition among the different oxidative and recombination routes. This is even more true for MILD and oxy-fuel combustion, where the effect of highly diluted conditions overcomes the effect of pre-heating, leading to an increase of characteristic times of fuel ignition and oxidation and a change in the relative weight of different kinetic pathways with respect to standard conditions. The same approach allowed for recent identification of methane cool flames [4,5] and dynamic phenomenologies obtained experimentally and numerically in a perfect stirred reactor [6,7] similar to the ones already well identified for high molecular weight hydrocarbons oxidation.

Recently, Picarelli et al. [8] have performed experimental campaigns on methane Mild combustion in a tubular flow reactor at atmospheric pressure. They valued auto-ignition delay times and found out a Negative Temperature Coefficient (NTC) behavior. Such

phenomenology is extensively described in the literature for C5–C7 paraffin [9] but few experimental evidences are present in the literature about the occurrence of such a behavior for methane oxidation. In addition, they have been generally observed in a pressure range of interest for engine or gas turbine, as summarized in a recent database published by Davidson and Hanson [10]. For instance, shock-tube experiments on methane ignition under engine-relevant conditions were carried out by Huang et al. [11]. Experimental analysis detected NTC phenomenology for mixtures of methane diluted in nitrogen and argon at moderate temperatures (1000–1350 K) and elevated pressure (16–40 atm). Analogously, an earlier work of Petersen et al. [12] reports about a change in activation energy by changing the temperature in the range between 1040 K and 1500 K at high pressure (40–260 atm). Sokolov et al. [5] report sparse experimental data carried out in a stirred reactor for CH_4/O_2 mixture in rich condition for inlet temperatures between 740 and 820 K at low pressures. Such experimental results can, in addition, hardly be used in evaluation or tuning kinetic models because experimental conditions have not been clearly reported in the paper. At higher temperature, the same authors detected methane cool flame behavior followed by an NTC phenomenology. Bendtsen et al. [13] also identify a NTC region when NO_x were added to $CH_4/O_2/H_2O$ mixture.

For the most part of the cited works the authors also attempted to establish a correspondence between experimental evidences and numerical simulations by modifying kinetic models available in the literature. However, in general a full satisfying correspondence between numerical and experimental data could not be achieved. For instance, Huang et al. [11] reached a good agreements between experimental and numerical data at stoichiometric and lean conditions adding reactions and modifying rate coefficients of Petersen mechanism [12]. But the model was not able to predict the experimental data at rich conditions. In turn, Petersen et al. [12] tuned the GRI-Mech 3.0 mechanism succeeding in modeling their experimental results but at the same time affirming that several reactions of methane ignition mechanism have rate coefficients that either have not ever been measured or are not well known. They demonstrated the kinetic importance of methyl peroxy radicals in describing methane ignition at very high pressures and intermediate temperatures, i.e. at the conditions that would emphasize pressure-dependent addition reactions, such as the ones that lead to CH_3O_2. They added methylperoxy radical kinetics to the GRI and those low T, high P reactions produced the inflection in the ignition delay times that the experiments demonstrated.

The aim of the present work is to compare the efficacies in predicting the existence of Negative Temperature Coefficient (NTC) behavior of ignition time of methane at atmospheric pressure of the main kinetic models available in the literature.

In this perspective, the autoignition delay time of methane air mixture have been evaluated in dependence of temperature by using several reaction mechanisms as available on the web. In addition, analyses of reaction pathway with several techniques have been carried out in order to highlight the kinetic controlling steps of methane autoignition in different temperature ranges.

2. Numerical methods

Numerical simulations for studying the evolution of methane ignition process at atmospheric pressure in diluted conditions were performed by means of PLUG application of the Chemkin 3.7 [14] software. PLUG simulates the behavior of plug-flow chemical reactor. Several oxidation kinetic mechanisms, freely available on the web, were considered. The names used to identify them in the paper along with the relative reference and the numbers of involved species and reactions are reported in Table 1 ([11,12,15–20]).

All these mechanisms were validated for a wide range of operative conditions and different reactor configurations in standard conditions, as well described in the literature.

In the present work, from the computed temperature axial profiles auto-ignition delay times (τ_{ign}) were assessed in a wide range of parameters. In particular, the investigated temperature range is 700–1500 K for a dilution of 85%, and with several carbon/oxygen (C/O) feed ratios at atmospheric pressure.

Following a criterium described in details elsewhere [21] τ_{ign} was defined as the time corresponding to a temperature increase of 10 K with respect to mixture inlet one (T_{in}).

In addition to auto-ignition delay computation, PLUG application has also been used for reaction sensitivity and rate of production analyses, whilst Cantera [22] was specifically used for automatically drawing net reaction path diagrams.

3. Results

3.1. Comparison of kinetic mechanisms

The prediction of the auto-ignition delay time (τ_{ign}) obtained with all the considered kinetic mechanisms have been reported in Figs. 1 and 2. Fig. 1 shows the Arrhenius plots of numerical auto-ignition delay times versus $1000/T_{in}$ (α) computed, at C/O = 0.2, with five of the seven selected mechanisms. All of them shows that auto-ignition delay decreases monotonically with temperature increase, linearly or nearly linearly. It has to be noted that the values predicted at each temperature span over a wide range of values. Autoignition delay time profiles computed with GRI-Mech 3.0 (double-dashed) and Konnov (solid line) envelop, upward and downward respectively, all the other profiles. For instance, at T_{in} = 830 K the values span over one order of magnitude, from the 50 s predicted by GRI-3.0 to the 3 s computed using Konnov mechanism. The variation is smaller at higher temperature. For T_{in} = 1250 K GRI-3.0 predicts a τ_{ign} = 0.02 s while Konnov mechanism gives a τ_{ign} = 0.008 s.

Profiles obtained with RAMEC, Warnatz and San Diego mechanisms lie between GRI-Mech 3.0 and Konnov lines. Warnatz and San Diego profiles lie in the lower value range closer to the Konnov one than to the GRI-Mech 3.0 one. RAMEC profile is closer to GRI-3.0 one at higher inlet temperature whereas it bends toward Konnov profile at lower temperature.

Fig. 2 shows autoignition delay obtained using Ranzi and Huang mechanisms. The gray area, reported in the figure, represents the region delimited by the GRI-Mech 3.0 and Konnov profiles reported in Fig. 1. It has been reported in order to facilitate the comparison among all the mechanisms. The two curves reported on the Arrhenius plot of Fig. 2 falls within or nearby such a region. Both mechanisms are able to predict the existence of temperature ranges related to different system reactivity. More specifically, both curves show that τ_{ign} decreases with temperature increase for

Table 1
Denomination, reference and numbers of involved species and reactions of the kinetic models used in this work.

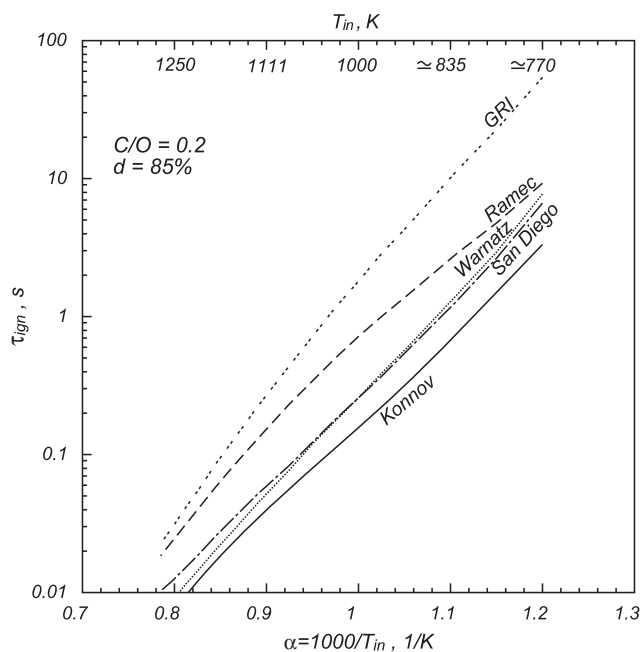| Model	Reference	# Of species	# Of reaction
Ranzi	[15]	69	1134
GRI-Mech 3.0	[16]	53	325
Warnatz	[17]	35	164
Huang	[11]	40	194
RAMEC	[12]	47	190
Konnov	[18]	127	1207
San Diego	[19]	46	235
Zhukov	[20]	209	1260

Fig. 1. Comparison of auto-ignition delay time computed with different kinetic mechanisms.
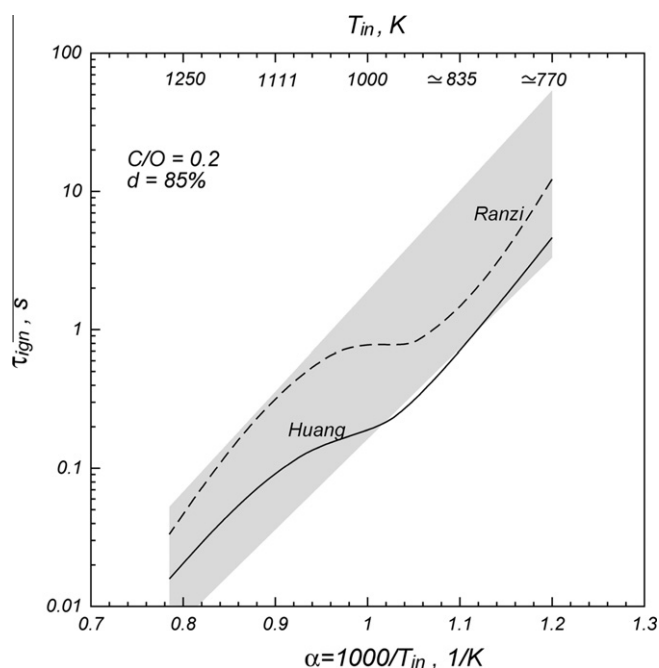

Fig. 2. Comparison of auto-ignition delay time computed with Huang and Ranzi mechanism. Gray area is the variation region of the ignition delay reported in Fig. 1.

temperature lower than 925 K and higher than 1050 K. For the intermediate range of inlet temperatures, between 925 K and 1050 K, the auto-ignition delay times curves show a change in slope which testifies a variation of system reactivity. Namely, for data obtained with Ranzi mechanism, τ_{ign} decreases of one order of magnitude, from 10 s to 1 s increasing T_{in} from 830 K to about 910 K, then it is nearly constant for a temperature change of about 120 K, from 910 K to 1010 K. Thereafter, τ_{ign} decreases linearly from 0.7 s to 0.015 s, with increasing T_{in} from 1070 K to 1265 K. The Huang mechanism produces lower auto-ignition delay times and a much smoother transition between the two regions of linear dependence on T_{in} with respect to the Ranzi one.

The trend evidenced in Fig. 2 by both curves recalls the well known Negative Temperature Coefficient (NTC) largely characterized by paraffins larger than C4. Generally, in the literature NTC region always refers to a range of temperature where ignition delay time increase with temperature, i.e. the slope of τ_{ign} as a function of $1000/T_{in}$ in an Arrhenius plot from positive becomes negative. In most cases here reported the change in slope is drastic because from a positive value it becomes nearly equal to zero, but it does not assume negative values. In the same conditions Petersen et al. [12] as well as Sokolov et al. [5] referred this region as NTC. Following the available literature, NTC acronym has been used hereafter in order to easily associate it to a change in slope of τ_{ign} as a function of $1000/T_{in}$ in a more general sense. As already described in Section 1, such a behavior is not fully characterized for low molecular weight hydrocarbon because there are very few experimental evidences showing a clear change in the reactivity of such hydrocarbons in any particular temperature range. This is most likely the reason why most of the mechanisms considered in this work are not able to predict its existence. As a matter of a fact, in the experimental facilities generally used for auto-ignition studies the fast ignition reactions hide the slower ones, characteristics of the intermediate temperature range, due to the nonuniform distribution of temperature typically occurring in those systems [15].

It is clear that an NTC behavior of methane auto-ignition cannot be associated to the same kinetic pathway that determines the occurrence of an NTC in high molecular weight paraffins oxidation because no oxygen double addition occurs in methane oxidation. In order to understand the chemical pathways controlling the autoignition delay time dependence on T_{in}, the Ranzi mechanism has been used for carrying out reaction path diagrams, sensitivity and rate of production analyses. It has been preferred to Huang mechanism because it shows a more defined NTC region. In addition it has been validated in a wider range of conditions and reaction configuration at atmospheric pressure.

4. Reaction path diagrams

In order to clarify the prevailing methane oxidation kinetic pathways at different temperature ranges, an extensive numerical simulation activity was carried out by means of Cantera software. First, simulations were run in order to compare ChemKin and Cantera results on the basis of temperature axial profiles and auto-ignition delay times. The results show that the software predictions are practically coincident.

Path diagrams, freezing the reaction network at $t = \tau_{ign}$, referred to carbon atoms for three different inlet temperatures and for C/O = 0.2 are shown in Figs. 3–5. Inlet temperatures have been chosen as representative of the three different ranges of temperature previously identified. Arrow thickness is proportional to the net reaction rates and the plot scale is equal to 10^{-4} mol/s/cm^3.

The reaction path diagram of Fig. 3 shows that, at T_{in} = 850 K, methyl radicals, formed by dehydrogenation from methane, are then oxidized to CH_3O and CH_3O_2. Later on, formaldehyde, formyl radical and CO are produced. At such an early stage of combustion the subsequent oxidation of CO to CO_2 is not active yet. The net reaction rates are relatively low.

At T_{in} = 975 K, in the temperature region where the results obtained using the Ranzi mechanism exhibit an NTC region, net reaction rates are higher with respect to the first case. In particular they result to be about six times the net rates relative to the previous considered temperature. Carbon main pathways are similar to the previous case even though two additional reactions routes are identifiable in the diagram reported in Fig. 4. Methyl radicals not only react following the oxidation channel to form CH_3O and
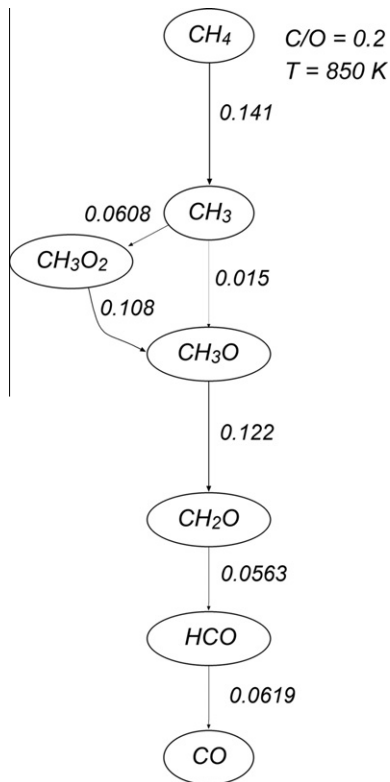
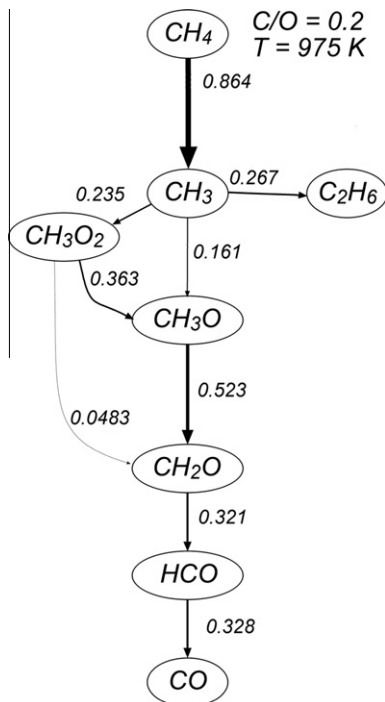**Fig. 3.** Flow diagram computed with Ranzi mechanism at 850 K.

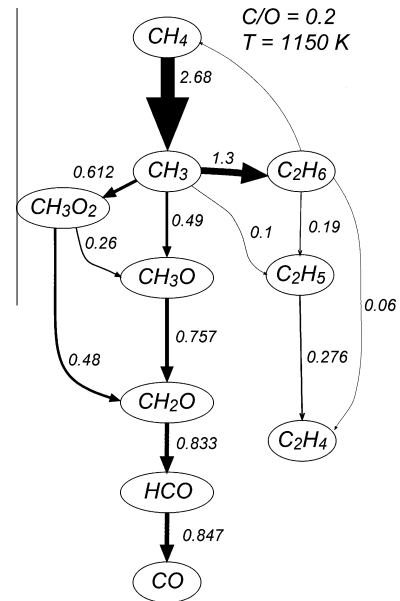**Fig. 4.** Flow diagram computed with Ranzi mechanism at 975 K.

Fig. 5. Flow diagram computed with Ranzi mechanism at 1150 K.

A further increase of T_{in} beyond the NTC region strongly enhances the methane conversion and, as a consequence, the subsequent reactions, as well shown in Fig. 5, obtained for 1150 K. As expected, the temperature affects also the relative weight of each channel. About 50% of methyl radicals feed the recombination channel. In addition, the formation of unsaturated hydrocarbons is set on. C_2H_5 radicals derive both by recombination from CH_3 radicals and by dehydrogenation from ethane. Then, they are dehydrogenated to ethene. The oxidation route follows the same channel reported for lower temperatures, even though the formation rate of CH_3O_2 and CH_3O from methyl radicals are, in this case, nearly equivalent. In addition the methyl peroxide radical decomposition to CH_2O and OH overcomes the metathesis of CH_3O_2 and CH_3 to form CH_3O. Similarly to the lower temperature cases, methoxy and methyl peroxide radicals are dehydrogenated to CO.

Relevant information can be earned by sensitivity analyses diagram of Figs. 6–8. obtained at 850 K, 975 K and 1150 K, respectively, at the relative ignition time. Summarizing the results for the three temperatures, the most sensitive reactions involved in the methane auto-ignition for the operative conditions considered can be listed as follow.

For the H_2/O_2 system main reactions are:

$$H + O_2 + M \rightarrow HO_2 + M \tag{1}$$

$$HO_2 + HO_2 \rightarrow H_2O_2 + O_2 \tag{2}$$

$$H_2O_2 + M \rightarrow OH + OH + M \tag{3}$$

$$H + O_2 \rightarrow OH + H \tag{4}$$

while for methane:

$$CH_4 + H \rightarrow CH_3 + H_2 \tag{5}$$

$$CH_4 + HO_2 \rightarrow CH_3 + H_2O_2 \tag{6}$$

$$CH_4 + O_2 \rightarrow CH_3 + HO_2 \tag{7}$$

The most sensitive reactions involving methyl radicals are:

$$CH_3 + HO_2 \rightarrow CH_3O + OH \tag{8}$$

$$CH_3 + O_2 = CH_3O + O \tag{9}$$

CH_3O_2, but also recombine yielding ethane. Furthermore, methyl peroxide leads to the formation not only of CH_3O, as at lower temperature, but also of formaldehyde and OH radicals. It is worth noting that about 75% of formed CH_3 is transformed in either CH_3O_2 or CH_3O, while the remaining 25% follows the recombination pathway, which subtracts carbon and hydrogen from oxidative channels.
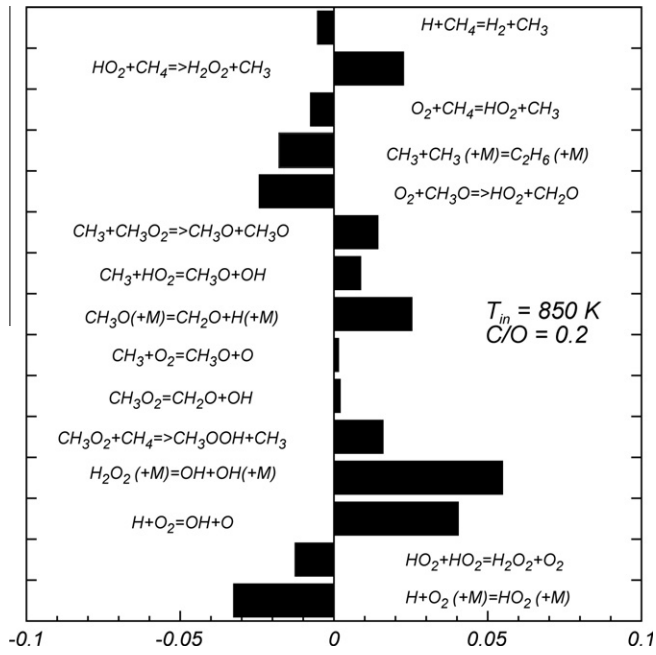
Fig. 6. Sensitivity coefficients obtained at 850 K and C/O = 0.2 with Ranzi mechanism.
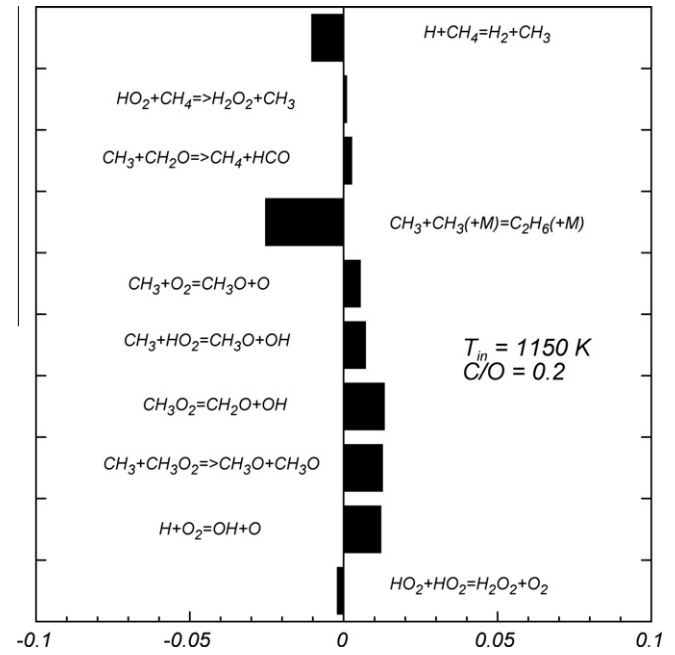

Fig. 8. Sensitivity coefficients obtained at 1150 K and C/O = 0.2 with Ranzi mechanism.
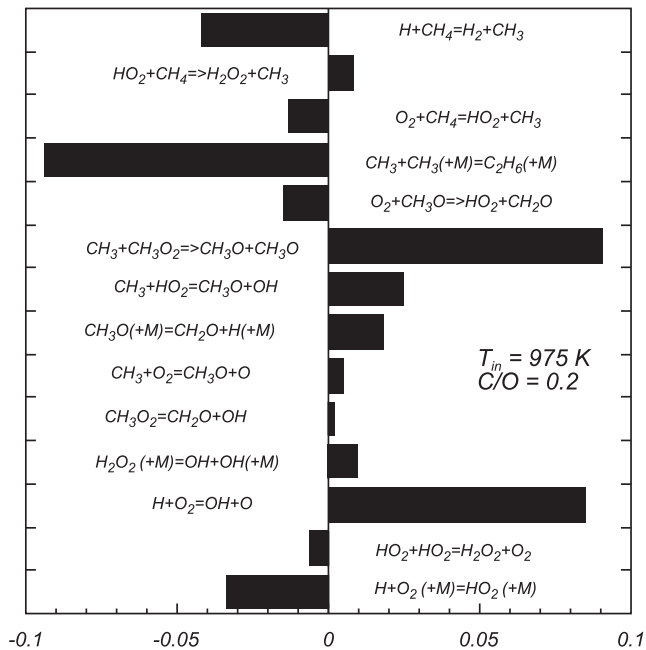

Fig. 7. Sensitivity coefficients obtained at 975 K and C/O = 0.2 with Ranzi mechanism.

$$CH_3 + CH_3O_2 \rightarrow CH_3O + CH_3O \qquad (10)$$

$$CH_3 + O_2 {=} CH_3O_2 \qquad (11)$$

$$CH_3 + CH_3 + M \rightarrow C_2H_6 + M \qquad (12)$$

while CH_3O and CH_3O_2 most relevant reactions are:

$$CH_3O + M \rightarrow CH_2O + H + M \qquad (13)$$

$$CH_3O_2 = CH_2O + OH \qquad (14)$$

$$CH_3O_2 + CH_4 \rightarrow CH_3OOH + CH_3 \qquad (15)$$

On the basis of information collected from path diagram and sensitivity analysis indications, the rate of production/destruction (ROP) of some key species involved in the most sensitive reactions has been analyzed as a function of temperature in Figs. 9 and 10.

The secondary axis of Fig. 9 shows the net rates of destruction of methyl radicals through the recombination route (reaction (12)) with dashed line and the sum of net rates of reactions that lead from methyl radicals to CH_3O and CH_3O_2 (namely from reactions (8)–(11)) with dashed-dotted line. On the same diagram the auto-ignition times of Fig. 1 has been reported in order to make easier the comparison of the different curves. The gray area highlights the temperature region of NTC.

It is worth noting that for low inlet temperatures the sum of methyl oxidation reaction rate increases as T_{in} increases. As soon as the recombination reaction becomes important, the oxidation reactions net rate increases with a lower slope, showing a maximum value just in correspondence of the beginning of the NTC temperature range, then it decreases slowly down to a relative minimum value. Later on, just after the NTC temperature range, it increases again increasing the temperature. The net rate of recombination reaction monotonically increases in the whole temperature range considered.

In order to identify the dominant branching reactions that lead to the main branching agent OH, relatively to the H_2/O_2 system, the rate of production of OH through the reaction (3) (hydrogen peroxide decomposition) and reaction (4) have been reported as function of $1000/T_{in}$ in Fig. 10 along with the auto-ignition delay time of Fig. 1.

For low temperatures the main branching mechanism is the decomposition of H_2O_2, while in the NTC range, the ROP of the reaction (3) shows a maximum just in correspondence of the low temperature side of the NTC region. Then, it decreases until the high temperature side of the NTC. Hereafter it increases due to the abruptly increase of reaction (4) that becomes the main branching reaction at high temperatures.

The correspondent diagrams of Figs. 9 and 10 obtained with GRI-Mech 3.0 have been summarized in Fig. 11. The rate of production of reactions (10) and (11) are missing because such reactions
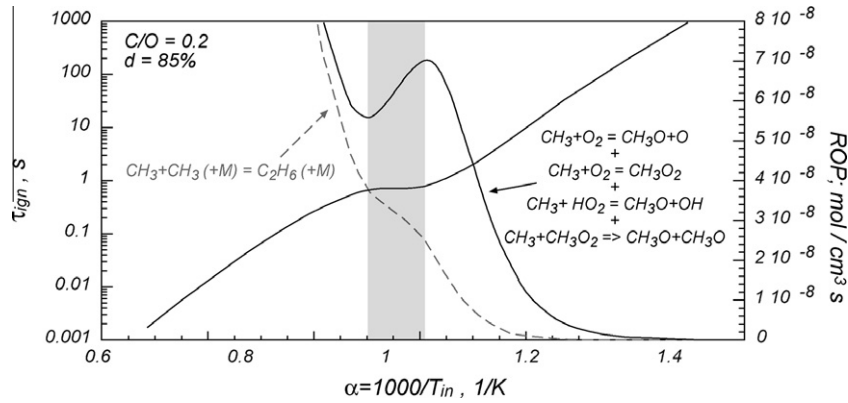
Fig. 9. Auto-ignition delay times and rate of production of CH_3 through oxidation and recombination channel.
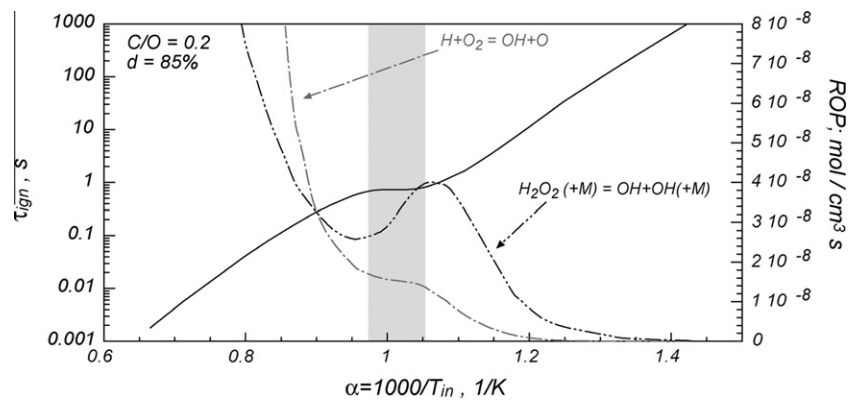

Fig. 10. Auto-ignition delay times and rate of production of OH reactions (3) and (4).
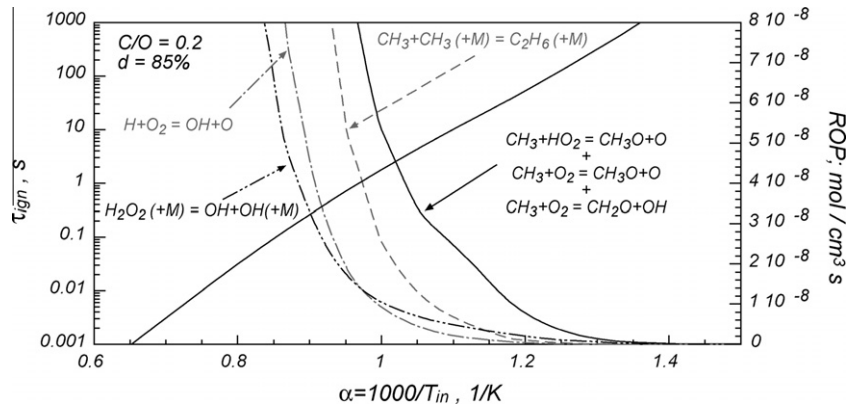

Fig. 11. Auto-ignition delay time and rate of production of specified reactions computed with GRI mechanism.

are not present in this mechanism. In consequence of their absence the rate of production of the other considered reactions show a monotonic increase with temperature with no remarkable trend. It has to be stressed that in this case the rates of production of reactions (3) and (4) do not differ as much as they do with the Ranzi mechanism.

5. Effect of mixture composition

The analysis of NTC behavior has been extended in order to evaluate the effect of mixture composition on ignition delay. More specifically two aspects have been taken into account that concern the effect of carbon to oxygen ratio and the nature of inert gas present in the reactive mixture. Therefore, numerical simulations were carried on by changing the mixture composition from lean to rich mixtures and by substituting nitrogen with different diluent species of interest in new combustion technologies.

Fig. 12 shows the auto-ignition time for three C/O, 0.1, 0.2 and 0.5. All the profiles show a similar trend. For inlet temperature lower than 850 K, the ignition delay is almost independent on carbon to oxygen ratio, while at temperature higher than 850 K the richer the mixture, the longer the auto-ignition time is. In addition, it is worth noting than the temperature ranges where an NTC behav-
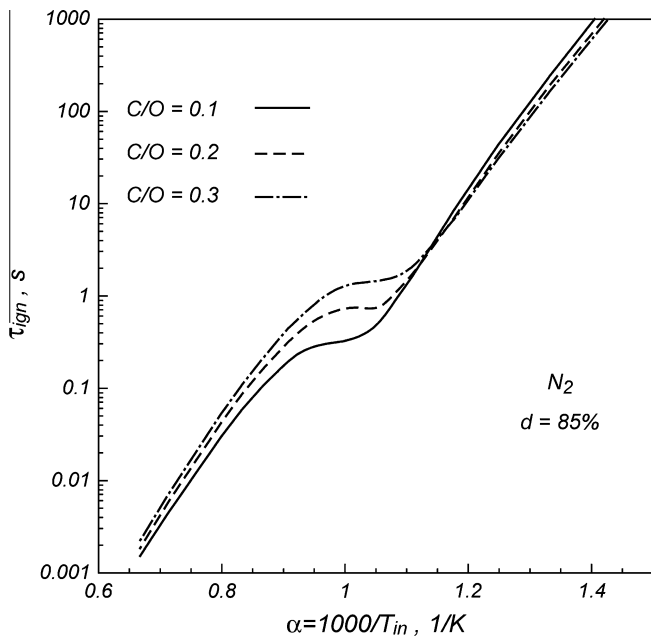
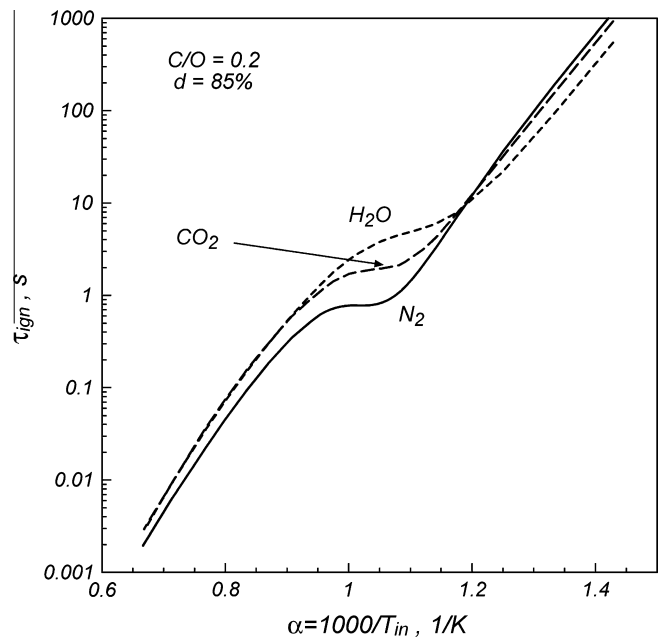**Fig. 12.** Auto-ignition delay time computed for three C/O ratio.

Fig. 13. Auto-ignition delay time obtained with different diluent species.

ior can be observed, in all the three considered cases, shift toward lower temperature values with increasing C/O feed ratio. At temperature above NTC regions ones differences among τ_{ign} values become more relevant.

Several numerical tests were carried out with different diluent species. Fig. 13 shows the auto-ignition delay times as function of $1000/T_{in}$ on curves parametric in the diluent, namely nitrogen, carbon dioxide and water vapor, for C/O = 0.2 and a dilution level equal to 85%.

The trend of curves is similar for all the cases. At low temperatures, for T_{in} value comprised between 700 K and 850 K, the shortest auto-ignition times competes to H_2O diluted system, while nitrogen diluted system shows the longest ones.

At T_{in} = 850 K curves intersect and, for T_{in} > 850 K, the trend is inverted and auto-ignition delay times computed using as diluents water and carbon dioxide are longer than those computed using N_2 as diluent. In particular, the longest auto-ignition times compete to the system diluted in water. For instance, at T_{in} = 1000 K, τ_{ign} is equal to 0.74 s for N_2, 1.69 s for CO_2 and 2.42 s for H_2O.

At T_{in} above 1100 K auto-ignition delay times computed for water and carbon dioxide diluted systems do not differ significantly.

6. Discussion

Comparison of the results of the previously reported kinetic analysis gives a straightforward indication of the steps controlling the ignition process in the temperature ranges where distinct behavior has been evidenced. Focusing the attention only on the first steps of oxidation process, three sets of reactions have been identified for the low, middle and high temperature ranges respectively.

For inlet temperatures lower than 925 K, methane is mainly oxidized to CO through the formation of CH_3O_2 by means of the equilibrium reaction (11). Then it rapidly forms $CH_3O \rightarrow CH_2O \rightarrow HCO \rightarrow CO$. In these conditions the main branching reaction is the decomposition of H_2O_2 to OH. The importance of the decomposition of H_2O_2 in providing chain branching and ignition at intermediate temperatures for low and high molecular weight

paraffins was explained by Westbrook [23]. The relevance of this path was also pointed out for high pressure range in shock tube by Petersen et al. [12].

The ratio among the different reaction channels changes by increasing the temperature. As a matter of facts, at intermediate temperatures the recombination path becomes active with a two-fold effect. It reduces CH_3 radicals available for the oxidation pathways thus shifting the equilibrium reaction (11) toward reactants and reducing the yield of methyl radical in CH_3O_2. In addition the reduced concentration of CH_3 lowers the rate of reaction (10), which is the main reaction channel of CH_3O_2 toward the final products.

These effects all result in a reduced system reactivity and an increase of auto-ignition delay times, thus producing an NTC behavior. In the same temperature range ignition is still mainly supported by H_2O_2 decomposition as branching reaction, even if reaction $H + O_2 \rightarrow OH + H$ gains relevance.

For higher inlet temperatures, above the NTC temperature range, the branching reactions that support the ignition are mainly the reaction $H + O_2 \rightarrow OH + H$ and the thermal decomposition of CH_3O_2. Such reactions enhance system reactivity and reduces the effect of auto-ignition times from the recombination channel. However, this chemical route plays a relevant role, storing carbon and hydrogen atoms in C_2 species, in this temperature range too.

The analysis on diluents effect confirms at some extent this scenario. Diluents affect the evolution of methane oxidation mainly acting on third body molecular reactions. As matter of fact the third body efficiency in ter-molecular reactions is higher for CO_2 and H_2O with respect to N_2. For instance, the efficiency of water in reaction (1) is 18 for water, 2.4 for carbon dioxide and only 1.26 for nitrogen. Therefore, at lower temperatures, carbon dioxide and water accelerate reactions (1) and (3) leading to a shorter auto-ignition time with respect to nitrogen. Likewise, the auto-ignition delay times of system diluted in water is much lower than that diluted with carbon dioxide since its third body efficiency is significantly higher.

When inlet mixture temperature increases, also reaction (12) is promoted by diluent third-body efficiencies causing a slowing down of system reactivity and longer auto-ignition times, as Fig. 3 shows. At high temperature the presence of water and carbon

dioxide stresses the competition between reactions (1) and (4), accelerating reaction (1), leading to slower auto-ignition times with respect to nitrogen. In particular way it is worth noting, in Fig. 11, that reaction (4) is not relevant for the system diluted in water.

Further simulations have been run setting the CO_2 and H_2O third-body efficiency coefficients equal to N_2 in the key ter-molecular reactions identified in the paper. Auto-ignition delay times resulted nearly coincident, confirming the hypothesis that the diluent nature affects the evolution of the oxidation process exclusively by means of third-body efficiency coefficients.

7. Conclusions

The analysis reported in the present paper has a twofold significance, related both to the process itself and to the numerical tools that are nowadays available for foreseeing its evolution in ideal and real systems.

Such as shown in other works [6], multi-channel fuel oxidation that occurs in nonstandard conditions highlights peculiar characteristics and dependence on process parameters different from the well assessed behavior of traditional processes. The change of characteristic times of specific reaction channels, due to the change of operative conditions, indeed influences the competitions among the different reaction channels producing unexpected effects. In the case of methane combustion, the multiple oxidation paths compete with recombination channel in consuming the fuel molecule. The prevalence of either the oxidation or the recombination results in a speeding or a slowing down of the reactive process. In this reactive network, a key role is covered by the active oxidation pathway. At the same time, in dependence of working temperature, the branching routes of H_2/O_2 reaction mechanism supply a great part of radicals needed for ignition. Thus, numerical results presented in the paper clearly show that the Negative Temperature Coefficient region in the Arrhenius plot of methane ignition delay marks the shift from one principal reaction route to the others.

Beside, the overview of the most popular detailed kinetic mechanisms for methane oxidation showed that their reliability lacks when they are utilized to predict hydrocarbons oxidation process features in not-conventional operative conditions, despite their proved robustness in evaluating the behavior of conventional systems. Only two of the considered mechanisms are able to predict the presence of an NTC region in ignition delay of methane, even though sparse experimental evidences reported in the literature clearly evidenced its existence. The extreme working conditions related to the new combustion technologies (i.e. MILD or oxy-fuel combustion) seem to enforce the kinetic effects that lead to the NTC behavior.

As a consequence, it is even more evident the twofold need of basic experimental works carried out in the range of parameters of interest of new combustion technologies on simple reactors. On one hand they will clarify the behavior of systems working in such specific conditions. In addition, they will provide the experimental database useful for improving the performance of detailed kinetic mechanisms.

References

[1] Cavaliere A, de Joannon M. Mild Combustion. Prog Energy Combust Sci 2004;30(4):329–66.
[2] de Joannon M, Sabia P, Cavaliere A. Mild Combustion. In: Lackner M, Winter F, Agarwal AK, editors. Handbook of combustion. Wiley-VCH Verlag GmbH & Co.: Weinheim; 2010.
[3] Normann F, Andersson K, Leckner B, Johnsson F. Emission control of nitrogen oxides in the oxy-fuel process. Prog Energy Combust Sci 2009;35(5):385–97.
[4] Vanpee M. On the cool flames of methane. Combust Sci Technol 1993;93(1):363–74.
[5] Sokolov O, Parfenov YV, Arutyunov VS, Basevich VV, Vedeneev VL. Study of cool-fame phenomena during self-ignition of methane–oxygen mixtures. Russ Chem Bull 1996;45(10):2316–20.
[6] de Joannon M, Cavaliere A, Faravelli T, Ranzi E, Sabia P, Tregrossi A. Analysis of process parameters for steady operations in methane mild combustion technology. Proc Combust Inst 2005;30(2):2605–12.
[7] de Joannon M, Sabia P, Tregrossi A, Cavaliere A. Dynamic behavior of methane oxidation in premixed flow reactor. Combust Sci Technol 2004;176(5–6):769–83.
[8] Sabia P, de Joannon M, Ragucci R, Picarelli A, Cavaliere A. Negative temperature coefficient behavior for $CH_4/O_2/N_2$ diluted mixtures in a tubular flow reactor, Mugla, Turkey; 2010.
[9] Vanhove G, Petit G, Minetti R. Experimental study of the kinetic interactions in the low-temperature autoignition of hydrocarbon binary mixtures and a surrogate fuel. Combust Flame 2006;145(3):521–32.
[10] Davidson D, Hanson RK. Fundamental kinetics database utilizing shock tube measurements. In: 6th international conference on chemical kinetics, Gaithersburg, MD; 2005.
[11] Huang J, Hill PG, Bushe WK, Munshi SR. Shock-tube study of methane ignition under engine-relevant conditions: experiments and modeling. Combust Flame 2004;136(1–2):25–42.
[12] Petersen E, Davidson D, Hanson R. Kinetics modeling of shock-induced ignition in low-dilution CH_4/O_2 mixtures at high pressures and intermediate temperatures. Combust Flame 1999;117(1–2):272–90.
[13] Bendtsen A, Glarborg P, Dam-Johansen K. Low temperature oxidation of methane: the influence of nitrogen oxides. Combust Sci Technol 2000;151(1):31–71.
[14] Kee R, Rupley FM, Miller JA, Coltrin ME, Grcar JF, Meeks E, et al. CHEMKIN collection, release 3.6. San Diego, CA: Reaction Design Inc.; 2000.
[15] Ranzi E, Faravelli T, Frassoldati A, Cuoci A. CRECK modeling. <http://creckmodeling.chem.polimi.it/C1C31006.CKI>;2010.
[16] Bowman C, Frenklach M, Gardiner WR, Smith G. The GRI 3.0 chemical kinetic mechanism. Berkeley, CA: University of California; 1999.
[17] Warnatz J, Maas U, Dibble R. Combustion: physical and chemical fundamentals, modeling and simulation, experiments, pollutant formation. Berlin: Springer Verlag; 2006.
[18] Konnov A. Mechanism ver. 0.5. <http://homepages.vub.ac.be/~akonnov/science/mechanism/main.html>; 2010.
[19] Williams F. <http://maeweb.ucsd.edu/~combustion.cermech>.
[20] Zhukov V. Kinetic model of alkane oxidation at high pressure from methane to *n*-heptane. Combust Theor Model 2009;13(3):427–42.
[21] de Joannon M, Cavaliere A, Donnarumma R, Ragucci R. Dependence of autoignition delay on oxygen concentration in mild combustion of high molecular weight paraffin. Proc Combust Inst 2002;29(1):1139–46.
[22] <http://code.google.com/p/cantera/>.
[23] Westbrook CK. Chemical kinetics of hydrocarbon ignition in practical combustion systems. Proc Combust Inst 2000;28(2):1563–77.